

Supporting Information

Molecularly Imprinted Polymer Colloids Synthesized by Miniemulsion Polymerization for Recognition and Separation of Nonylphenol

Emile Decompte,[†] Volodymyr Lobaz,[‡] Mathilde Monperrus,[†] Elise Deniau,[†] Maud Save*[†]

[†] CNRS, University Pau & Pays Adour, E2S UPPA, Institut des Sciences Analytiques et de Physico-Chimie pour l'Environnement et les Matériaux, IPREM, UMR5254, 64000, PAU, France.

[‡] Institute of Macromolecular Chemistry AS CR, Heyrovsky Sq. 1888/2, 162 06 Prague 6, Czech Republic.

Mail: maud.save@univ-pau.fr

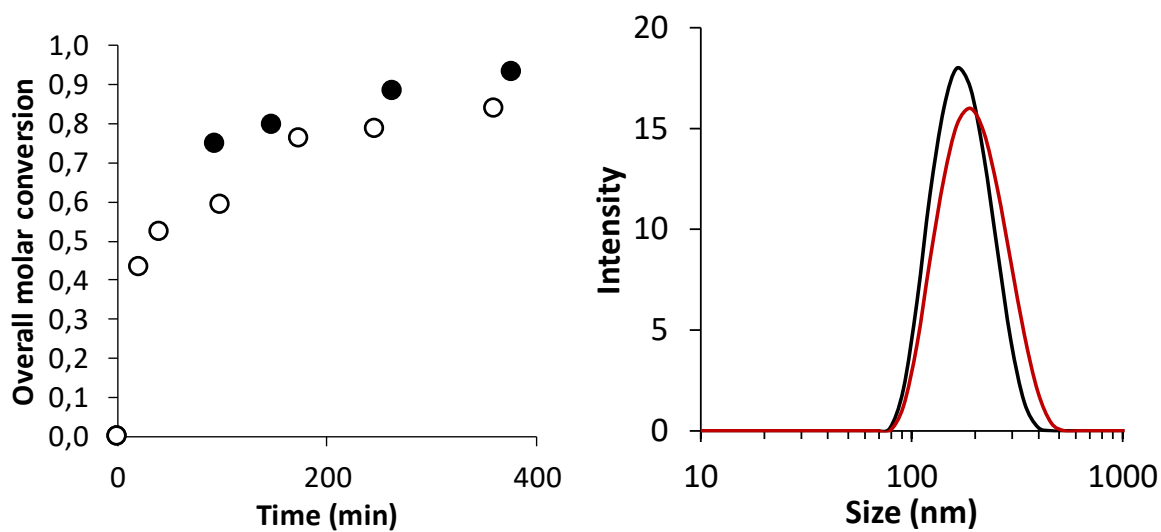


Figure S 1. Overall molar monomer conversion as a function of polymerization time for duplicated syntheses of MIP-VAc₁₇-VCL₁₇-DVA₆₆ with the corresponding size distributions determined at 0.05 g.L⁻¹.

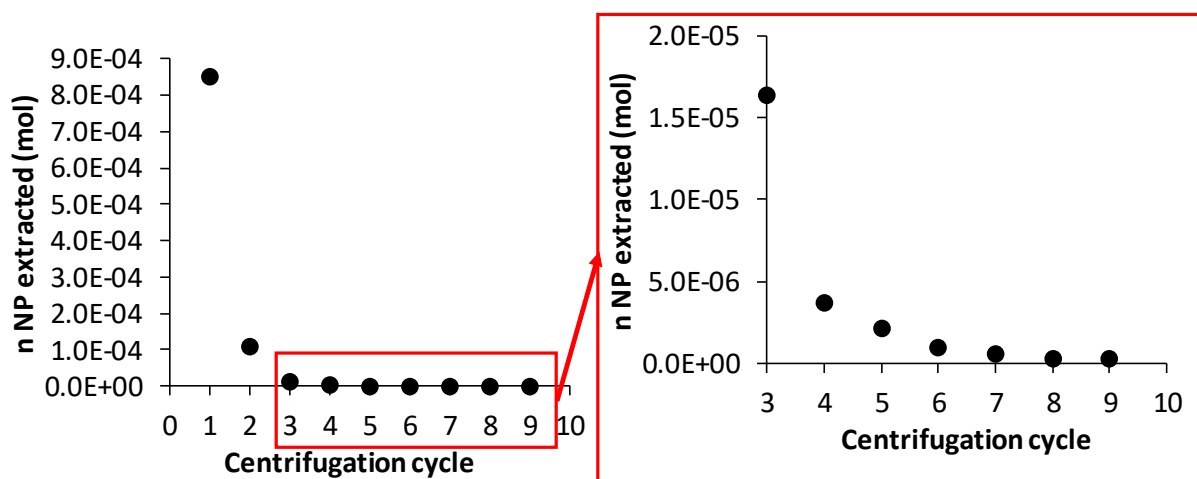
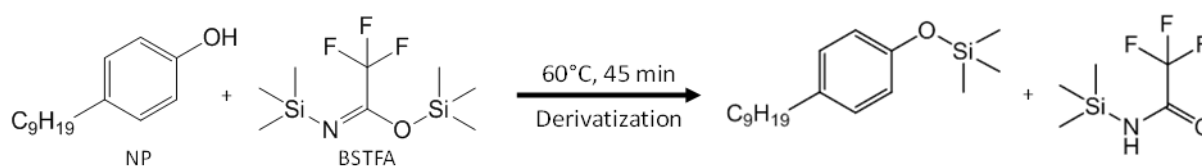


Figure S 2. Number of moles NP extracted after each centrifugation cycle with ethyl acetate for the MIP-DVA₁₅-VCL₄₂-VAc₄₃.

Liquid-liquid extraction of the nonylphenol in water, derivatization step and quantification of extracted NP by GC-MS analysis.

To measure the residual concentration of the NP in water, it is necessary to extract NP with an organic solvent because the aqueous phase cannot be directly injected into GC-MS. Different liquid-liquid extractions were attempted in order to select the most suitable organic solvent. The protocol was as follows: 500 μl of the aqueous NP solution are mixed with 500 μl of the organic solvent in a 2 mL Eppendorf tube. The mixture was sonicated for 3 minutes and then vortexed for 5 minutes before being left to decant.

Prior to quantitative GC-MS analysis of the NP, a trimethylsilylation derivatization of NP was performed as follows (Scheme S1): 125 μL of the NP solution were mixed with 50 μL of *N,O*-Bis(trimethylsilyl)trifluoroacetamide (BSTFA) and the mixture was placed in an oven for 45 min at 60°C: ¹⁻³



Scheme S1: Chemical reaction involved in the derivatization process of the NP prior to GC-MS injection.

The extraction yield (r) was calculated from Eq S. 1.

$$r (\%) = \frac{C_{NP \text{ extracted}}}{C_{NP \text{ initial}}} \times 100$$

Eq S. 1

$C_{NP \text{ extracted}}$ (mol.L^{-1}) is the concentration of the NP in the organic phase after the extraction and C_0 is the initial concentration of the NP in water ($C_0 = 4.54 \mu\text{mol.L}^{-1} = 1 \text{ mg.L}^{-1} = 1 \text{ ppm}$). It is required to establish calibration curves in order to calculate $C_{NP \text{ extracted}}$. For that purpose, 20 μL of a reference solution of NP in isopropanol at 1004 ppm was poured into 20 mL of an organic solvent. Several solutions of NP at 0.5 ppm, 0.2 ppm, 0.1 ppm and 0.01 ppm were

prepared by dilution to plot the calibration curve of GC-MS area signal versus derivatized NP concentration. Calibration curves were performed directly in ethyl acetate, and in dichloromethane after extraction from water (**Figure S 3**).

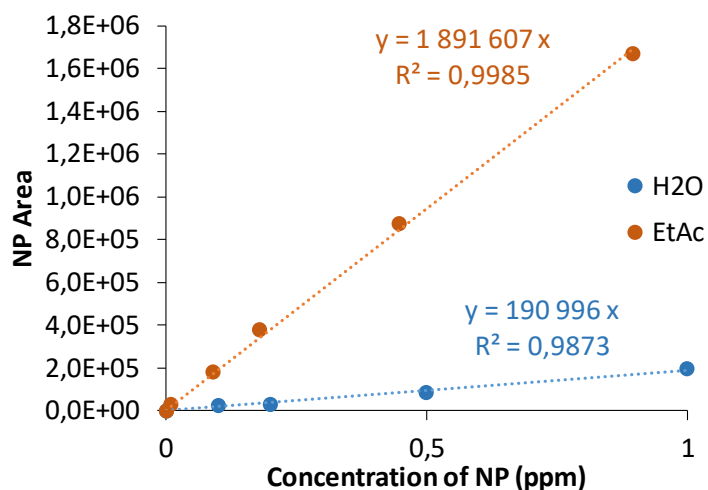


Figure S 3. Calibration curves for the NP in ethyl acetate (orange) and for the NP extracted with dichloromethane from water solutions (blue) of NP at 0.1, 0.2, 0.5 and 1 ppm for GC-MS analysis.

Ethyl acetate, isooctane and dichloromethane provided extraction yield of 4%, 55% and 94% respectively. Thus, dichloromethane was selected to extract NP from water samples and triplicate measurements provided an average NP extraction yield of 92 %. In order to provide an accurate measurement of NP present in water, the GC-MS peak area of derivatized NP extracted with dichloromethane was plotted against the concentration for 5 aqueous solutions of NP at 1 ppm, 0.5 ppm, 0.2 ppm, 0.1 ppm and 0.01 ppm.

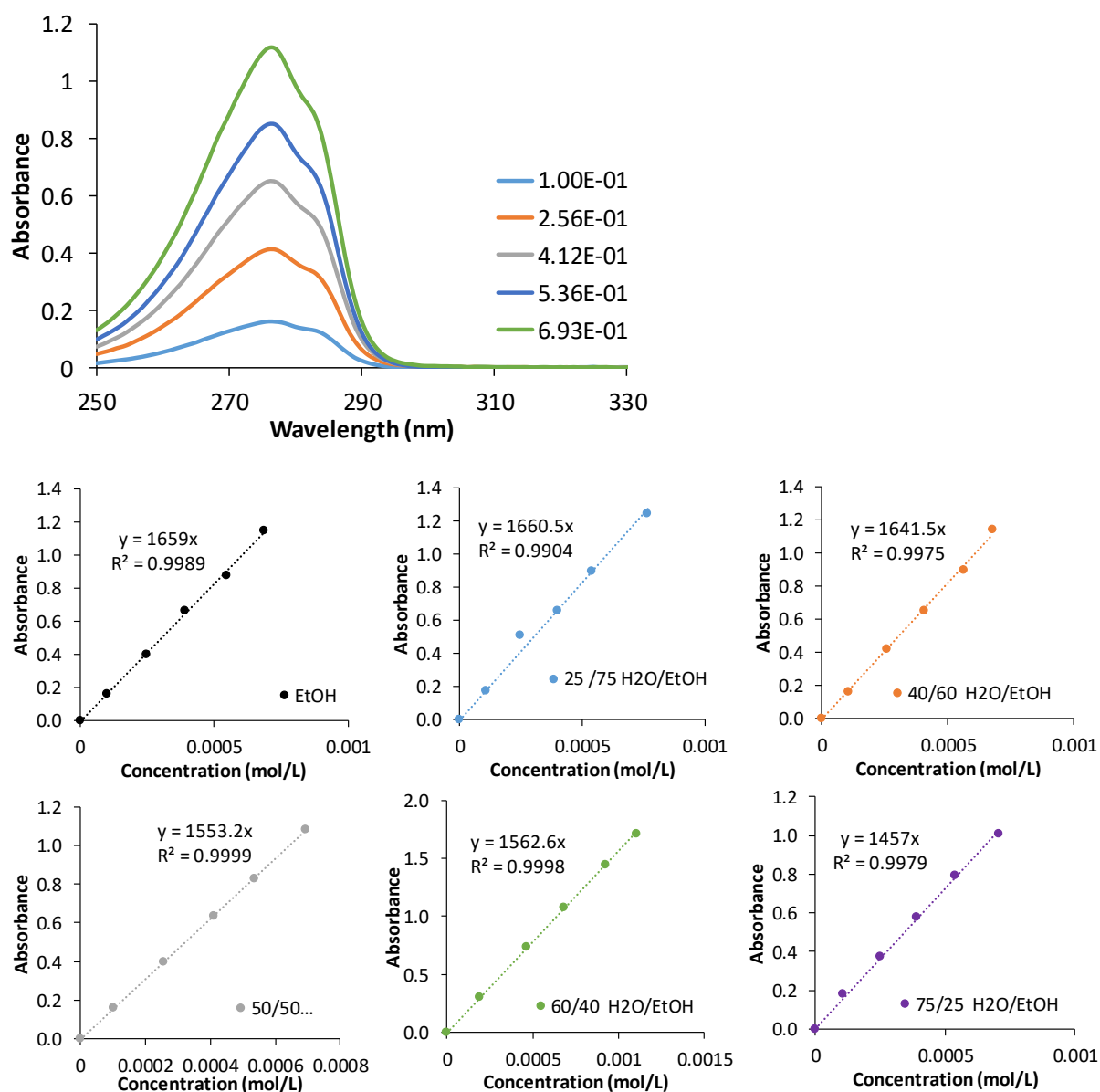


Figure S 4. Example of the absorbance spectra of NP in EtOH/water at various concentrations and calibration curves for NP in water/ethanol mixtures at different water content (H₂O/EtOH v/v). Spectra were recorded with a 1 cm long quartz cells with solution concentrated from 0.1 to 1.1 mmol.L⁻¹. The absorbance was monitored at 278 nm. The corresponding molar absorption coefficients (ϵ in L.mol⁻¹.cm⁻¹) corresponds to the slope of each linear plot.

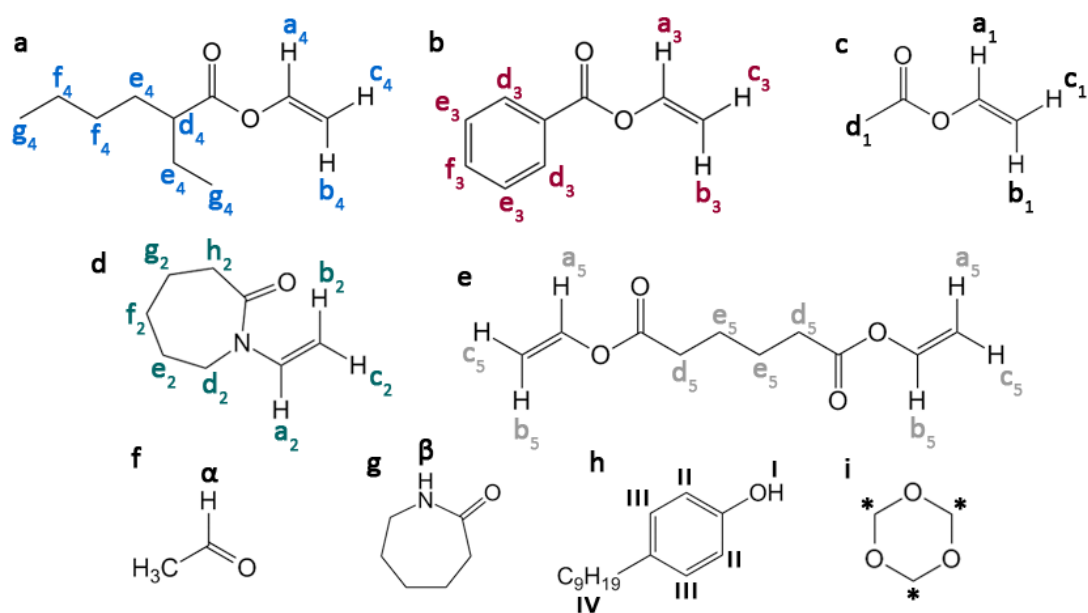


Figure S 5. Chemical structures of (a) 2-ethylhexanoate vinyl ester (VeOVAEH), (b) vinyl benzoate (VB) and (c) vinyl acetate (VAc) used as co-monomer, (d) *N*-vinylcaprolactam (VCL) used as functional monomer, (e) divinyl adipate (DVA) used as crosslinker, (f) acetaldehyde and (g) caprolactam used to monitor the hydrolysis of the VCL by ^1H NMR, (h) nonylphenol (NP) used as template and (i) trioxane used as internal standard to determine the double bond conversion by ^1H NMR.

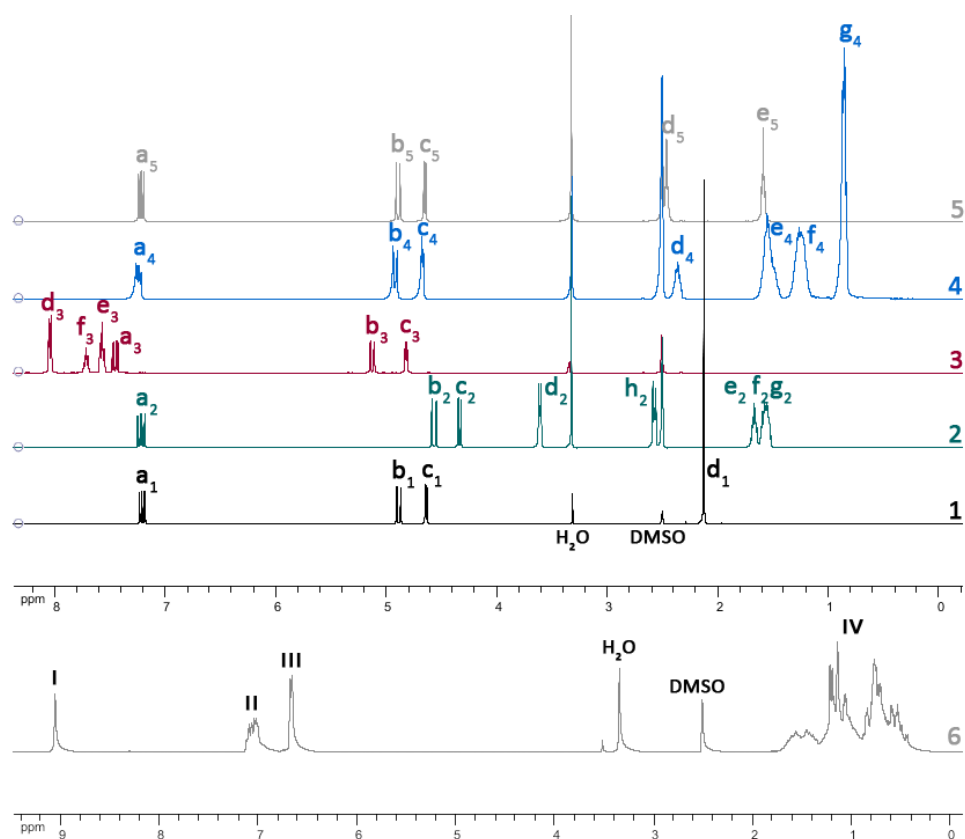


Figure S 6. ^1H NMR spectra of (1) vinyl acetate, (2) *N*-vinylcaprolactam, (3) vinyl benzoate, (4) 2-ethylhexanoate vinyl ester, (5) divinyl adipate and (6) nonylphenol in deuterated dimethylsulfoxide ($\text{DMSO-}d_6$) at room temperature.

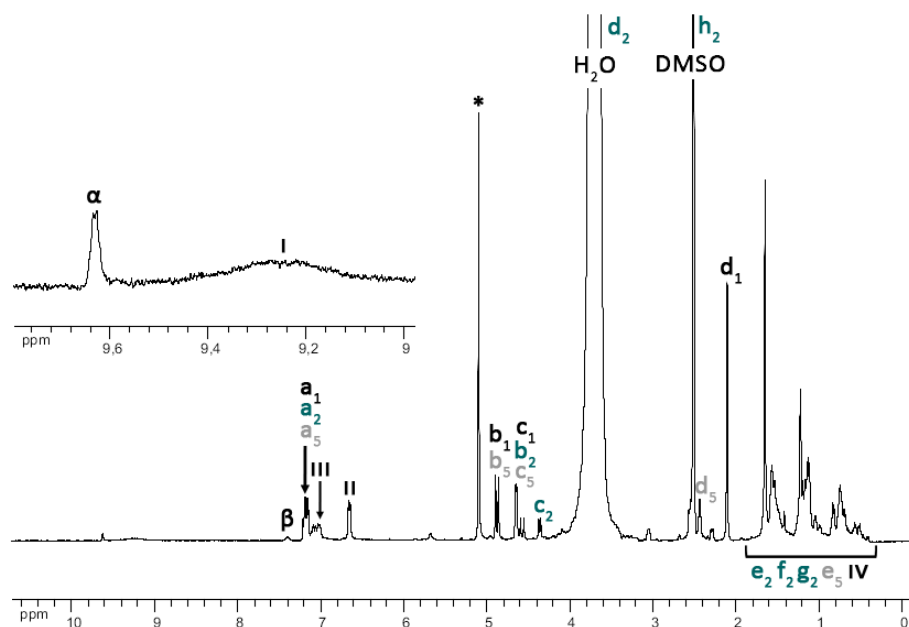


Figure S 7. ^1H NMR spectrum of a VAc/VCL miniemulsion (MIP-DVA₅₀-VCL₂₅-VAc₂₅) polymerization at $t = 270$ min in presence of nonylphenol in $\text{DMSO-}d_6$ at room temperature.

Optimization of miniemulsion polymerization of VCL/VAc/DVA in the absence (NIP) or presence (MIP) of nonylphenol.

The VCL/VAc/DVA miniemulsion polymerizations conducted at 65°C with 0.05 to 0.07 mol-% of AIBN (**Table S1**) ended up with low monomer conversion of about 40 % for 6h of polymerization while 90 % of monomer conversion were achieved in 5 hours by increasing AIBN content up to 0.10 mol-% (**Figure S 8**).

Table S1. Set up of the optimum experimental conditions for the miniemulsion copolymerization of VAc and VCL performed at 65°C with 10 wt-% of initial solids content.^a

Expt	f NaHCO ₃ ^b mol-%	f_{AIBN}^c mol-%	$\frac{[\text{NP}]_0}{[\text{VCL}]_0}$	X_m^d %	pH	r_{Hy}^e %	D_h^f nm	PDI ^f
NIP-AIBN _{0.07} -Buffer _{0.3}	0.3	0.07	0	40	4.1	29	na ^g	na ^g
NIP-AIBN _{0.05} -Buffer ₂	1.9	0.05	0	40	5.4	13	na ^g	na ^g
NIP-AIBN _{0.1} -Buffer ₂	1.9	0.11	0	69	5.4	15	282	0.20
NIP-AIBN _{0.1} -Buffer ₃	2.9	0.10	0	77	5.5	10	306 ^h	0.23
MIP-AIBN _{0.1} -Buffer ₂	1.8	0.10	0.25	22	4.1	22	na ^g	na ^g
MIP-AIBN ₂ -Buffer ₂	1.9	1.85	25	52	3.9	19	195	0.10
MIP-AIBN ₄ -Buffer ₂	1.9	3.93	25	75	3.6	10	176	0.06
MIP-AIBN ₈ -Buffer ₂	1.8	7.72	25	79	3.5	8	179	0.07

^a Experimental conditions: 6 mol-% DVA as cross-linker versus the total number of moles of monomers; molar fraction of the monomers : $f_{\text{VAc},0} = f_{\text{VCL},0} = 0.5$. ^b f_{NaHCO_3} is the molar fraction of buffer versus the total number of moles of monomers: $f_{\text{NaHCO}_3} = 100 \times n_{\text{NaHCO}_3} / (n_{\text{VAc}} + n_{\text{VCL}} + n_{\text{DVA}})$. ^c f_{AIBN} is the molar fraction of initiator versus the total number of moles of monomers and crosslinker: $f_{\text{AIBN}} = 100 \times n_{\text{AIBN}} / (n_{\text{VAc}} + n_{\text{VCL}} + n_{\text{DVA}})$. ^d X_m is the overall molar conversion of vinylic monomers and crosslinker at 6 h of polymerization, see **Erreur ! Source du renvoi introuvable.** ^e r_{Hy} is the hydrolysis yield of VCL. The hydrolysis yield (r_{Hy}) are calculated from by using the ratio of integrals of acetaldehyde at the end of polymerization and of the integral of the VCL measured at the initial time ($I_{1\text{H,VCL}}$ at 4.4 ppm, 1H) using I_{trioxane} as internal standard. ^f Hydrodynamic diameter (D_h) and polydispersity index (PDI) measured by DLS. ^g The conversion was too low so the diameter was not measured. ^h Low fraction of sedimented particles.

$$r_{\text{Hy}} (\%) = \frac{(I_{1\text{H}acetaldehyde})_t / (I_{1\text{H}trioxane})_t}{(I_{1\text{H}VCL})_0 / (I_{1\text{H}trioxane})_0} \times 100$$

Eq S. 2

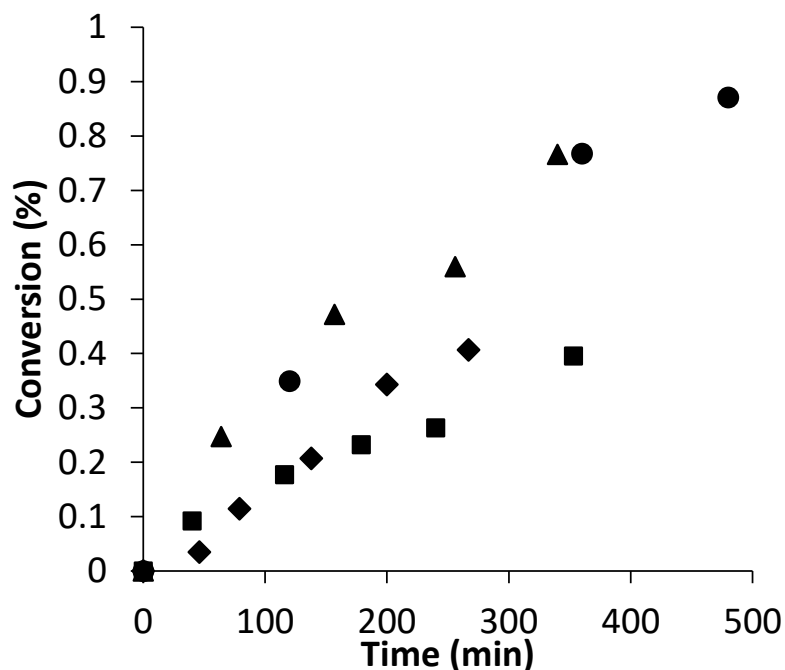


Figure S 8. Overall molar conversion of VAc, VCL and DVA versus polymerization for NP-free miniemulsion polymerization carried out at 65 °C at different molar fractions of AIBN initiator and NaHCO₃ buffer: (■) NIP-AIBN_{0.05}-Buffer₂, (◆) NIP-AIBN_{0.07}-Buffer_{0.6}, (●) NIP-AIBN_{0.1}-Buffer₂, (▲) NIP-AIBN_{0.1}-Buffer₃ (see Table S1).

Herein, sodium hydrogen carbonate buffer was used for the particle synthesis in order to counterpart the hydrolysis of the VCL. Indeed, Imaz *et al.*⁴ highlighted a noticeable VCL hydrolysis in acidic media, producing acetaldehyde and caprolactam, but the hydrolysis yield was significantly hindered in buffered aqueous phase. The yield of hydrolysis rate was decreased from 29 % for NIP-AIBN_{0.07}-Buffer_{0.3} to 13-15 % by increasing NaHCO₃ concentration up to 2-3 mol-% (NIP-AIBN_{0.1}-Buffer₂, NIP-AIBN_{0.1}-Buffer₃, see **Table S1**). It should be noticed that 3 mol-% of NaHCO₃ versus all led to the lowest yield of hydrolysis (10%). For all the series of NIP colloids synthesized with 2-3 mol-% of NaHCO₃ (corresponding to 4 to 6 mol-% of NaHCO₃ versus VCL), a monomodal particle size distribution was observed by DLS (**Figure S 11**). The average D_h of the initial monomer droplets was about 180 nm, which is lower than the final polymer particle diameter ranging from 280 to 310 nm suggesting slight monomer diffusion or particle aggregation during miniemulsion process (**Figure S 12**). In conclusion of this part, well-defined crosslinked P(VCL-*co*-VAc) NIP colloids dispersed in an aqueous phase are successfully synthesized by using 0.1 mol.-% of AIBN and 2 mol-% of buffer based on monomers.

We thus explored miniemulsion copolymerization of VCL, DVA and VAc in the presence of NP as template to prepare the imprinted colloids (**Table S1**). As mostly reported in the

literature, a fraction of 25 mol-% of nonylphenol versus the H-bonding VCL functional monomer was chosen. The polymerization rate was drastically reduced by the presence of the nonylphenol (**Figure S 9**), which was expected as the phenoxyl radicals formed from phenolic compounds are known as radical scavengers.⁵ Thus, a series of MIPs were synthesized with an increasing amount of initiator (from 0.1 mol-% to 8 mol-% vs. monomers) in order to determine the minimum concentration required to overcome this retardation (Figure S 9b and **Figure S 10**).

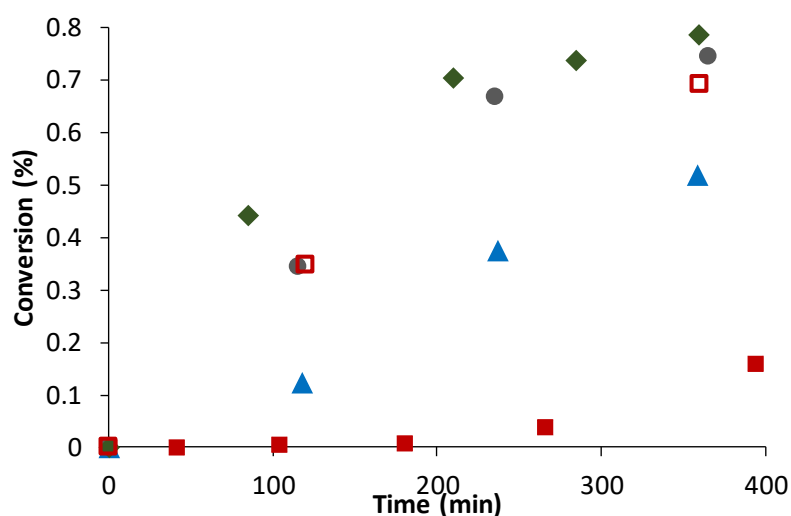


Figure S 9. Kinetics of miniemulsion copolymerization of VCL, VAc and DVA in the presence of 25 mol-% of NP based on VCL with various amounts of AIBN initiator: (■) MIP-AIBN_{0.1}-Buffer₂, (▲) MIP-AIBN₂-Buffer₂, (●) MIP-AIBN₄-Buffer₂, (◆) MIP-AIBN₈-Buffer₂ (see **Table S1**). Comparison with kinetics of miniemulsion polymerization in the absence of NP (□ NIP-AIBN_{0.1}-Buffer₂).

A concentration of 4 mol-% of AIBN based on monomers and crosslinker was sufficient to overcome the retardation and to reach a good level of monomer conversion of 75-80 %. Increasing the concentration up to 8 mol-% increased the initial polymerization rate but ending with a similar range of final monomer conversion. As the inhibition period is sharply reduced in the case of 2 – 8 mol-% of initiator, the nucleation time was lowered producing higher number of particles as the particle hydrodynamic diameter was in a lower range (180 – 195 nm) compared to NIP particles synthesized at 0.1 mol-% of initiator (**Table S1**). A faster droplet nucleation tends to reduce monomer diffusion across the water phase so the final particle diameter was in the range of the initial monomer droplets (180 nm, **Figure S 12**).

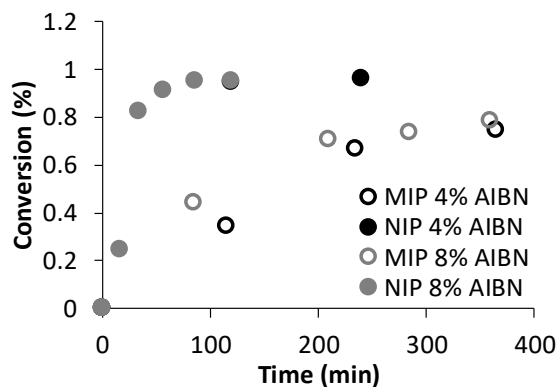


Figure S 10. Kinetics of the miniemulsion of VAc and VCL with 4 or 8 mol.-% of initiator in the presence (MIP) or absence (NIP) of nonylphenol. Polymerization temperature = 65°C, 14 mol.-% of DVA based on VCL, VAc and DVA and 25 mol.-% of NP vs. VCL.

Table S2: Weights of monomers, crosslinker and nonylphenol for MIP and NIP synthesized by miniemulsion polymerization

Expt. ^a	m co ^b	m VCL	m DVA	m NP
	(g)	(g)	(g)	(g)
NIP-DVA ₆ -VCL ₄₇ -VAc ₄₇	1.66	2.64	0.45	-
NIP-DVA ₁₅ -VCL ₄₂ -VAc ₄₃	1.45	2.25	1.21	-
NIP-DVA ₃₃ -VCL ₃₃ -VAc ₃₄	0.99	1.56	2.22	-
NIP-DVA ₅₀ -VCL ₂₅ -VAc ₂₅	0.67	1.07	3.13	-
NIP-DVA ₆₇ -VCL ₁₇ -VAc ₁₇	0.42	0.66	3.74	-
MIP-DVA ₆ -VCL ₄₇ -VAc ₄₇	1.64	2.67	0.45	1.03
MIP-DVA ₁₅ -VCL ₄₂ -VAc ₄₃	1.37	2.24	1.14	0.83
MIP-DVA ₃₃ -VCL ₃₃ -VAc ₃₄	0.97	1.67	2.22	0.66
MIP-DVA ₅₀ -VCL ₂₅ -VAc ₂₅	0.71	1.07	3.05	0.43
MIP-DVA ₆₇ -VCL ₁₇ -VAc ₁₇	0.42	0.67	3.88	0.28
NIP-DVA ₃₂ -VCL ₃₂ -VeoVA ₃₆	1.91	1.31	1.906	-
MIP-DVA ₃₄ -VCL ₃₃ -VeoVA ₃₃	1.63	1.31	1.951	0.51
NIP-DVA ₃₃ -VCL ₃₄ -VB ₃₃	1.51	1.43	1.97	-
MIP-DVA ₃₃ -VCL ₃₄ -VB ₃₃	1.51	1.37	1.96	0.57

Characterization of initial liquid miniemulsion and final dispersed polymer colloids by dynamic light scattering.

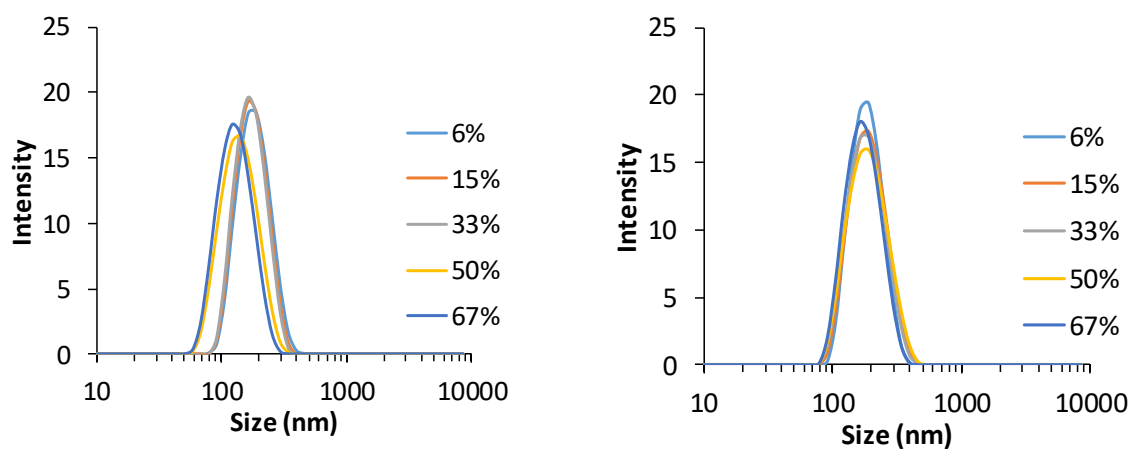


Figure S 11. Overlay of average particle size distribution measured by DLS in deionized water for a series of (Left) NIP-DVA-VCL-VAc colloids with various mol-% of crosslinker and (Right) MIP-DVA-VCL-VAc colloids with various mol-% of crosslinker. $[NIP] = [MIP] = 0.05 \text{ g.L}^{-1}$. $[NaHCO_3] = 4 \text{ mol-\%}$ of based on VCL.

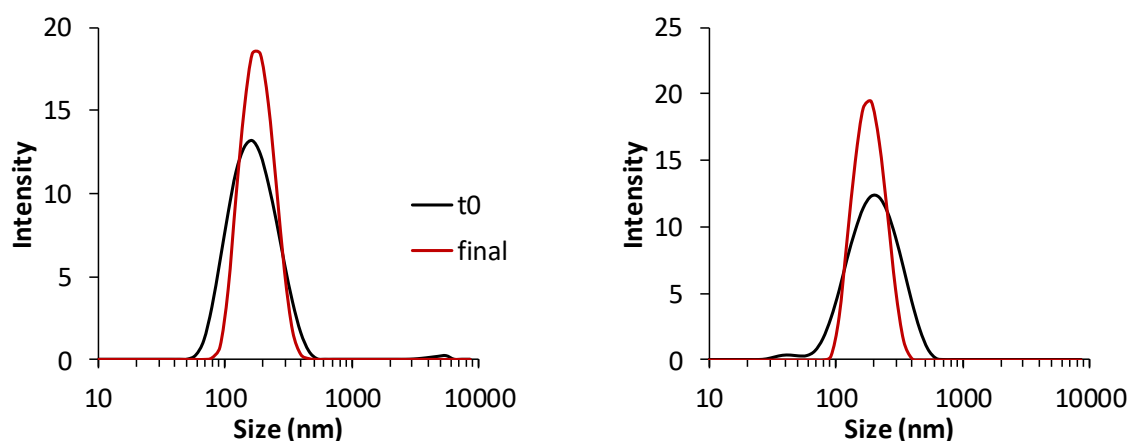


Figure S 12. Overlay of droplet size distribution (= initial liquid monomer droplets prior polymerization, $[DVA + VCL + VAc] = 100 \text{ g.L}^{-1}$) (black) and particle size distribution of the final polymer colloids (red, $[NIP] = 0.05 \text{ g.L}^{-1}$): Left) NIP-DVA₆-VCL₄₇-VAc₄₇ particles, Right) MIP-DVA₆-VCL₄₇-VAc₄₇.

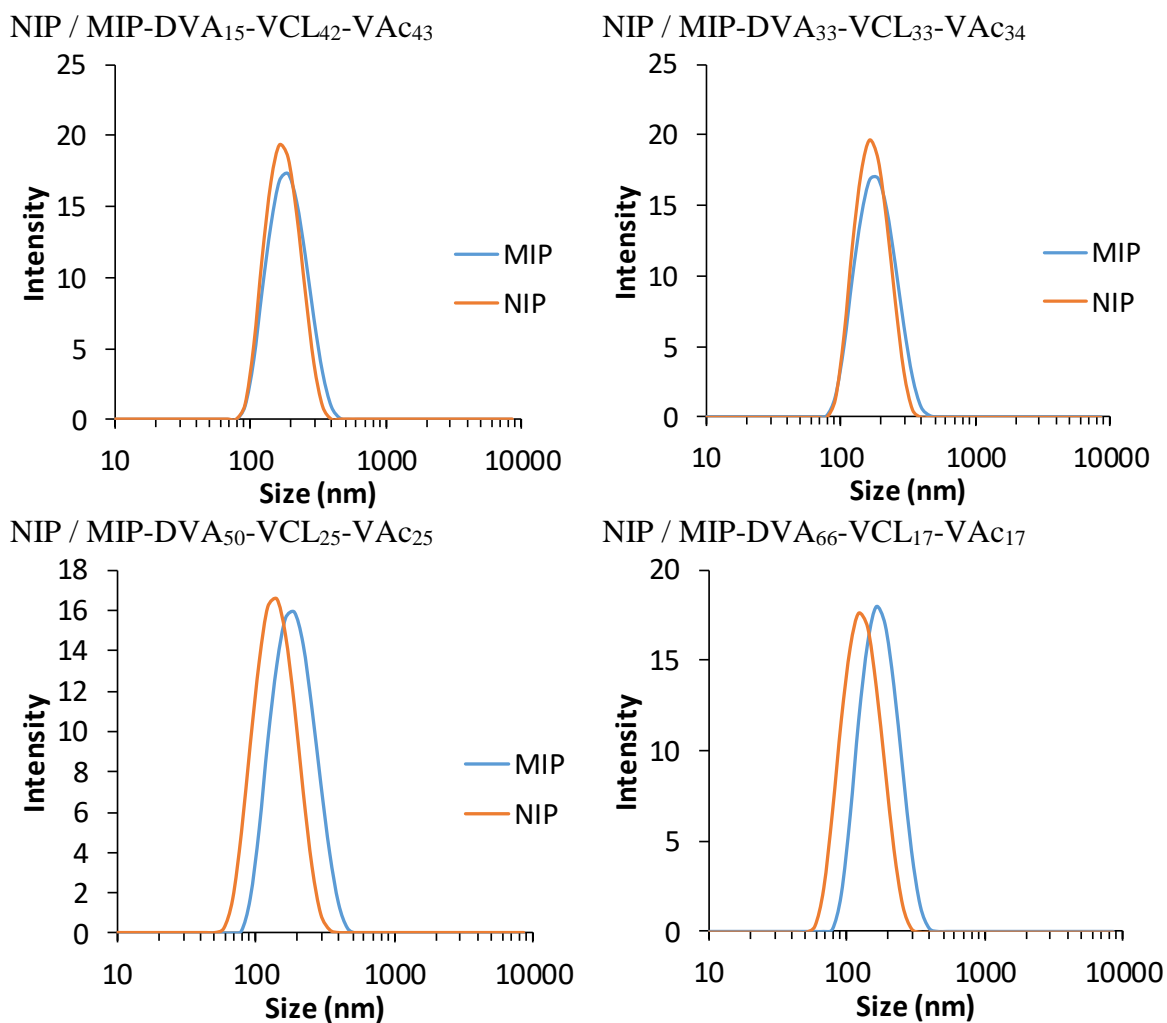


Figure S 13. Overlay of average particle size distribution measured by DLS in deionized water for each corresponding MIPs and NIPs. $[NIP] = [MIP] = 0.05 \text{ g.L}^{-1}$.

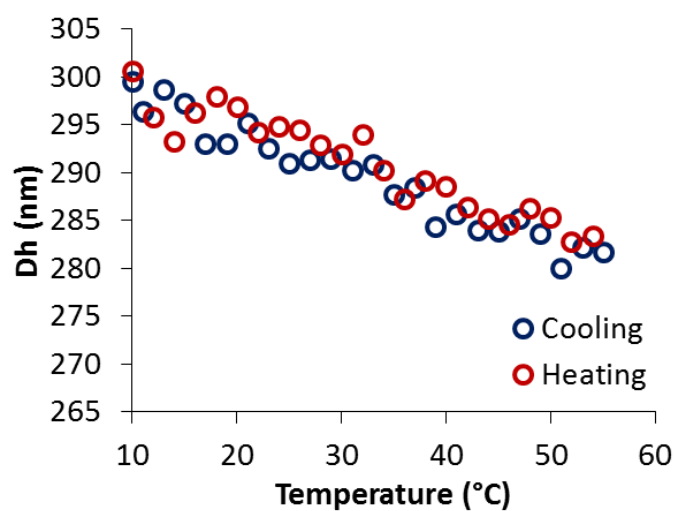


Figure S 14. Final average hydrodynamic diameters as a function of the temperature for NIP-DVA₆-VCL₄₇-VAc₄₇ colloids.

Table S3 : Hydrodynamic diameters and related polydispersities obtained for a series of MIPs and NIPs after dialysis and 11 months later. Measured at 0.05 g.L⁻¹.

Sample	After dialysis		After 11 months	
	Dh (nm)	PDI	Dh (nm)	PDI
NIP-DVA ₁₅ -VCL ₄₂ -VAc ₄₃	166	0.076	176	0.108
NIP-DVA ₃₃ -VCL ₃₃ -VAc ₃₄	163	0.074	171	0.111
NIP-DVA ₅₀ -VCL ₂₅ -VAc ₂₅	130	0.086	129	0.115
NIP-DVA ₆₇ -VCL ₁₇ -VAc ₁₇	122	0.08	126	0.11
MIP-DVA ₁₅ -VCL ₄₂ -VAc ₄₃	178	0.091	180	0.066
MIP-DVA ₃₃ -VCL ₃₃ -VAc ₃₄	174	0.094	178	0.081
MIP-DVA ₅₀ -VCL ₂₅ -VAc ₂₅	177	0.12	182	0.118
MIP-DVA ₆₇ -VCL ₁₇ -VAc ₁₇	164	0.084	168	0.078

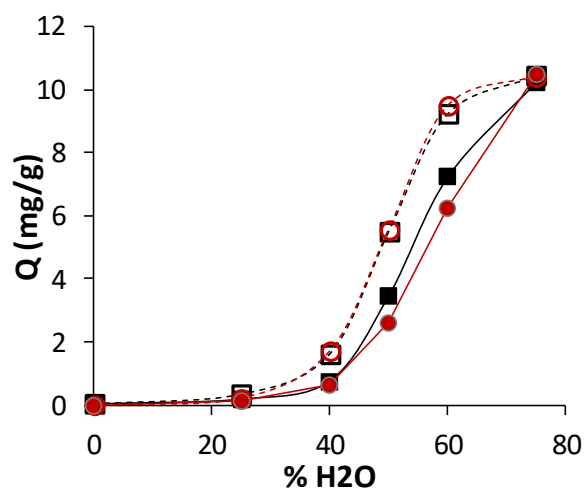


Figure S 15. Adsorption capacity of NP onto DVA₃₃-VCL₃₃-VAc₃₄ (black squares) and DVA₆₇-VCL₁₇-VAc₁₇ (red circles) MIP (empty symbols) and NIP (plain symbols) colloids as function of water fraction in the hydro-alcoholic solvent.

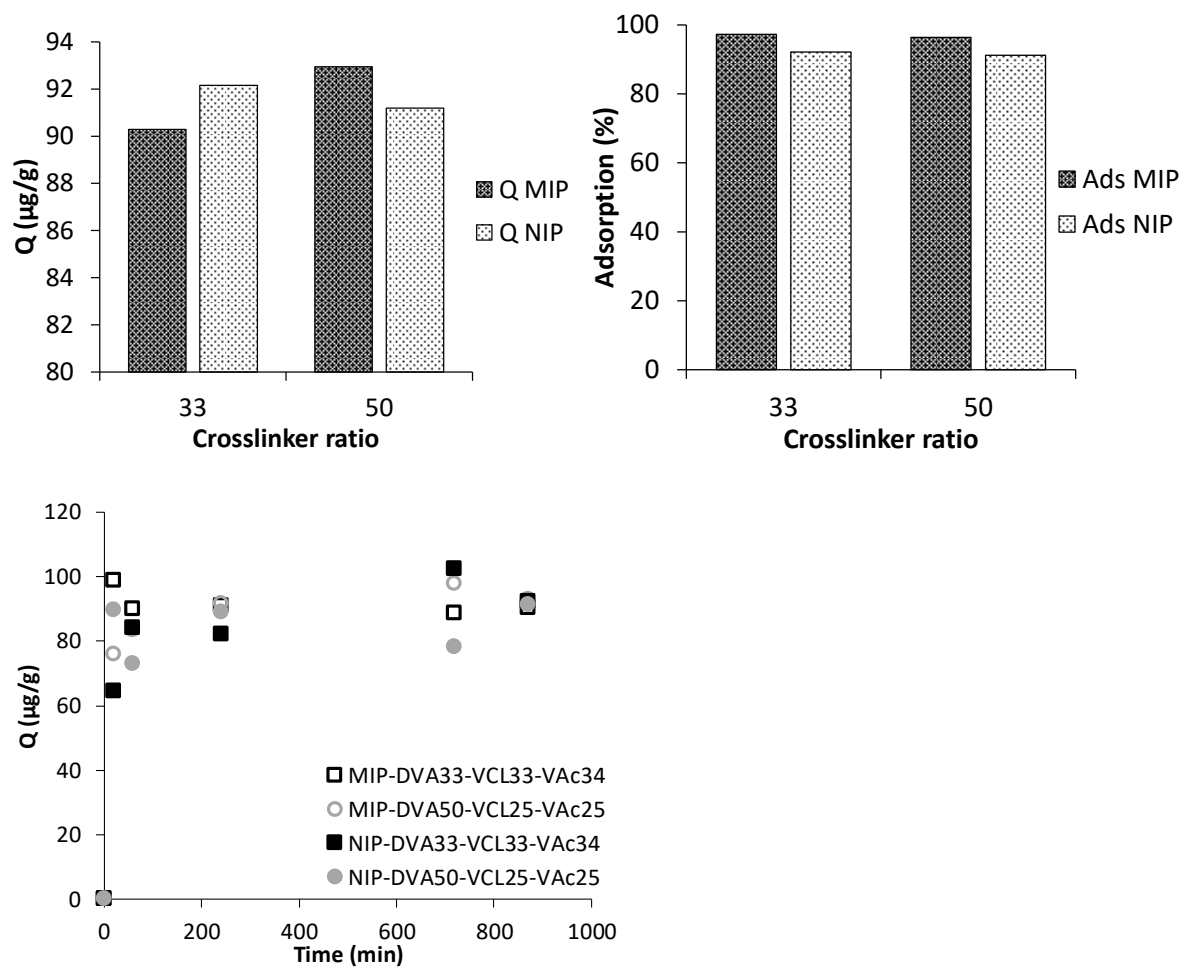


Figure S 16. Top) Adsorption capacities ($\mu\text{g/g}$) and adsorption yield, bottom) kinetics of the NP adsorption in 100 % water for MIP and NIP colloids synthesized with VAc as co-monomer and different DVA crosslinker ratios (in % based on VAc, VCL and DVA) . $[\text{NP}]_{0, \text{H}_2\text{O}} = 1 \text{ ppm}$ and $[\text{MIP}]_{0, \text{H}_2\text{O}} = [\text{NIP}]_{0, \text{H}_2\text{O}} = 10 \text{ g}\cdot\text{L}^{-1}$.

Table S4: Residual NP concentration in washed MIPs determined by GC-MS in ethyl acetate prior to adsorption experiment in H₂O. The initial concentration of NP used for the synthesis of MIP is on average 8 to 11 g.L⁻¹.

Sample	Centrifugation cycle	
	number	[NP] _{supernatant} (μg.L ⁻¹)
MIP-DVA ₆ -VCL ₄₇ -VAc ₄₇	19	32.55
MIP-DVA ₁₅ -VCL ₄₂ -VAc ₄₃	18	35.92
MIP-DVA ₃₃ -VCL ₃₃ -VAc ₃₄	20	28.03
MIP-DVA ₅₀ -VCL ₂₅ -VAc ₂₅	17	14.72

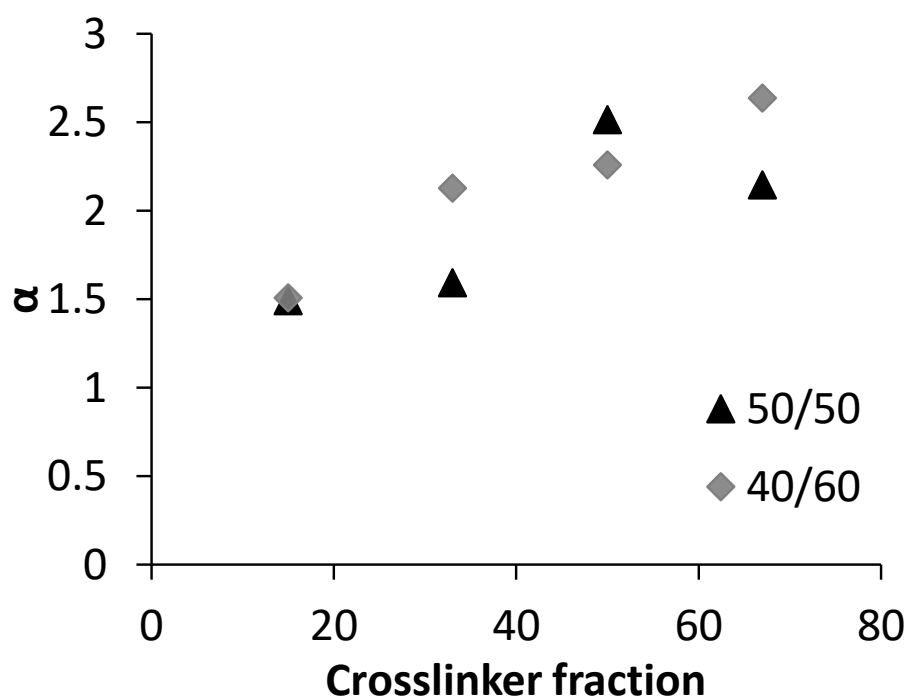


Figure S 17. Imprinting factors versus the molar DVA crosslinker fraction for NP adsorption carried out in 40/60 and 50/50 v/v H₂O/EtOH mixtures for DVA-VCL-VAc colloids.

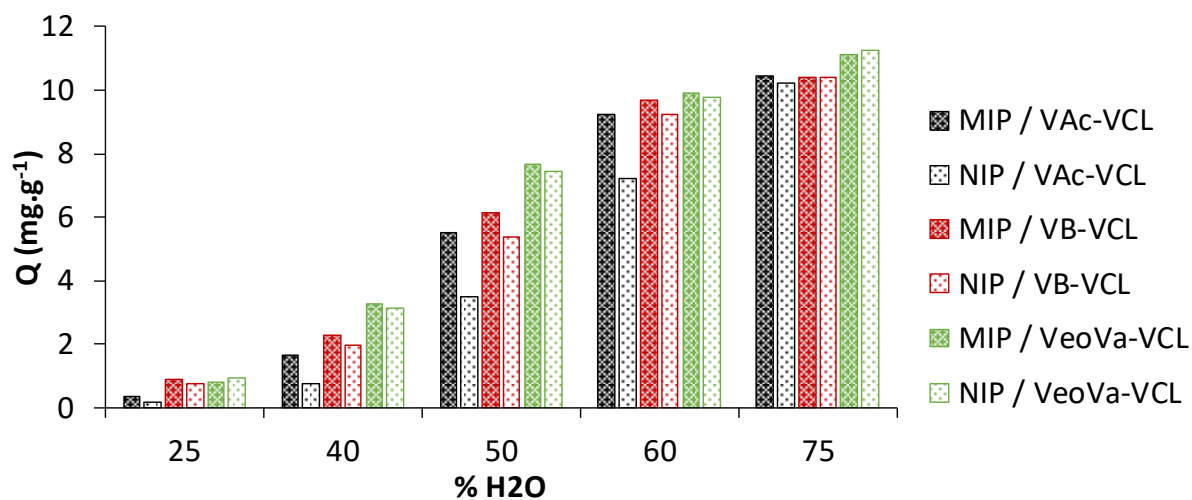


Figure S 18. Adsorption capacity (Q) for NP at different water contents of a series of NIP-DVA₃₃-VCL₃₃-M and MIP-DVA₃₃-VCL₃₃-M crosslinked with 33 % DVA, with M = VAc, VB or VeoVA co-monomer. Adsorption of NP ($[NP]_0 = 0.5 \text{ mmol.L}^{-1}$, 110 ppm) in EtOH/H₂O 50/50 v/v for $[MIP]_0 = [NIP]_0 = 10 \text{ g.L}^{-1}$.

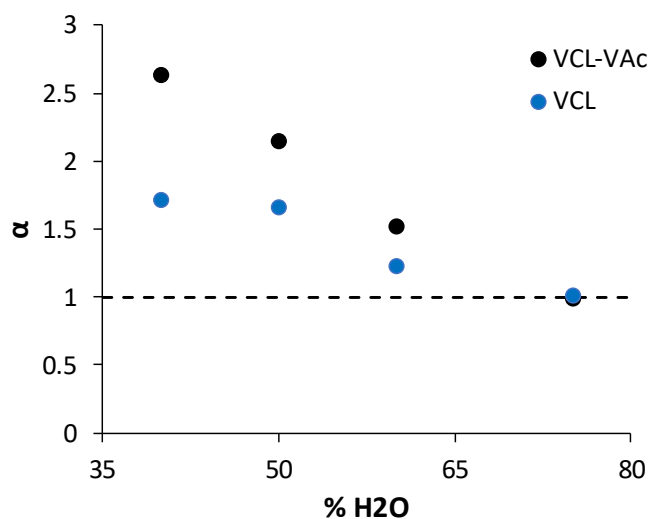
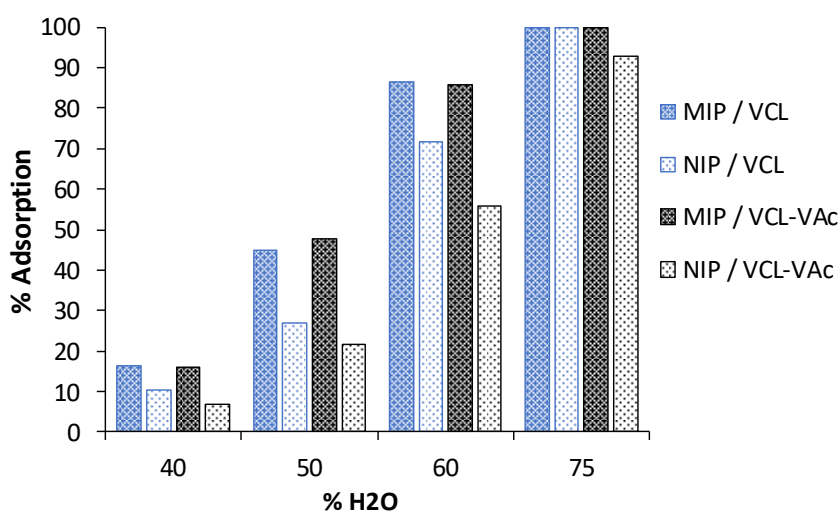
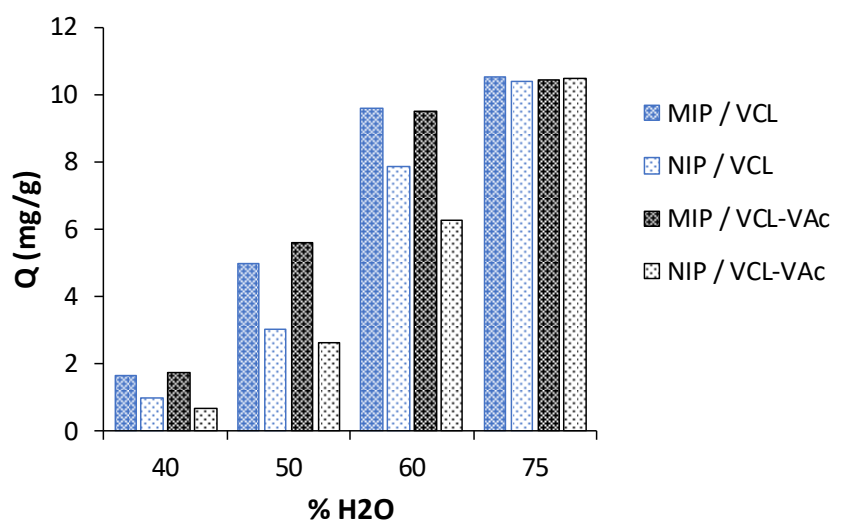


Figure S 19. Comparison of the adsorption capacity (Q) (**top**), adsorption yield (**middle**) and corresponding imprinting factor (α) (**bottom**) at different water contents for NIP and MIP crosslinked with 66 % of DVA: PVCL-based MIP and NIP (Blue, DVA₆₆-VCL₃₄) or P(VCL-VAc)-based MIP and NIP (Black, DVA₆₆-VCL₁₇-VAc₁₇). Adsorption of NP ($[NP]_0 = 0.5 \text{ mmol.L}^{-1}$, 110 ppm) for $[MIP] = [NIP]_0 = 10 \text{ g.L}^{-1}$.

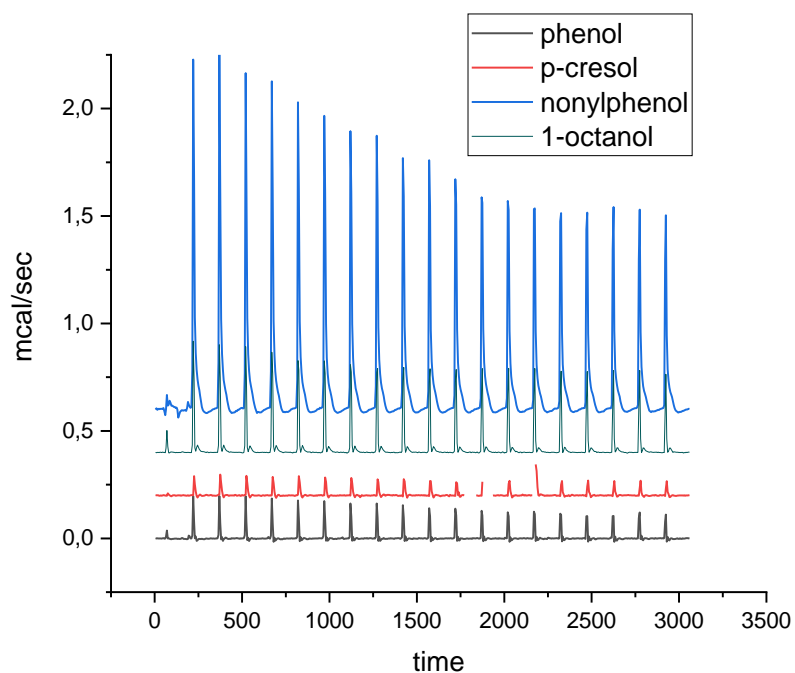


Figure S 20. Comparison of ITC traces for titration 20 mM of different injectants with ethanol/water 50/50 v/v at 25°C. Injectants are Nonylphenol, octanol, *p*-cresol and phenol.

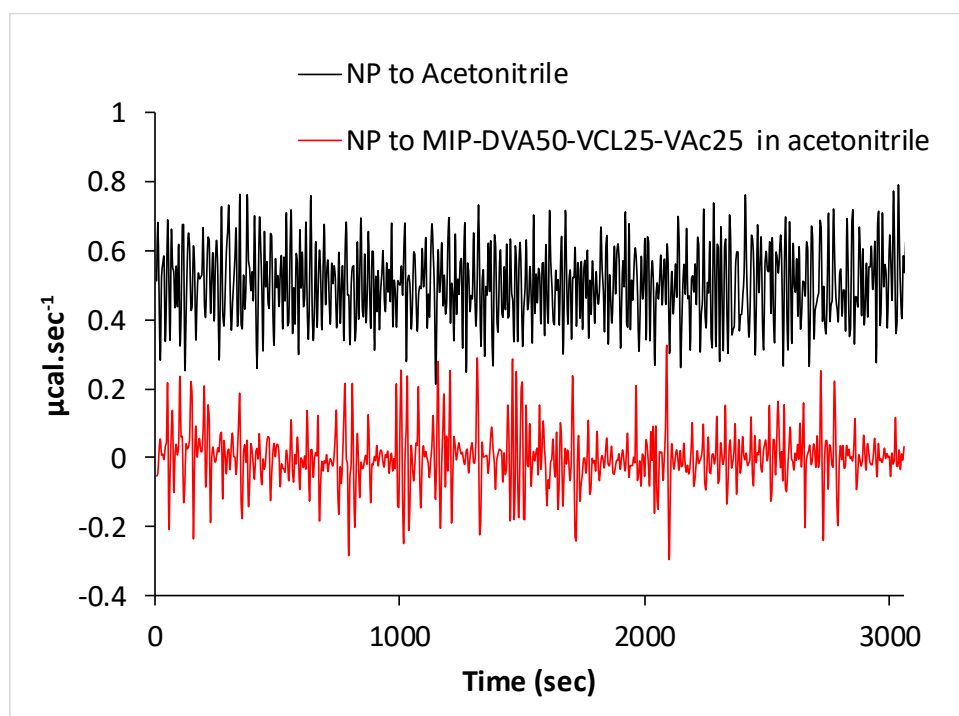


Figure S 21. Titration of NP with acetonitrile and with MIP-DVA₅₀-VCL₂₅-VAc₂₅ in acetonitrile

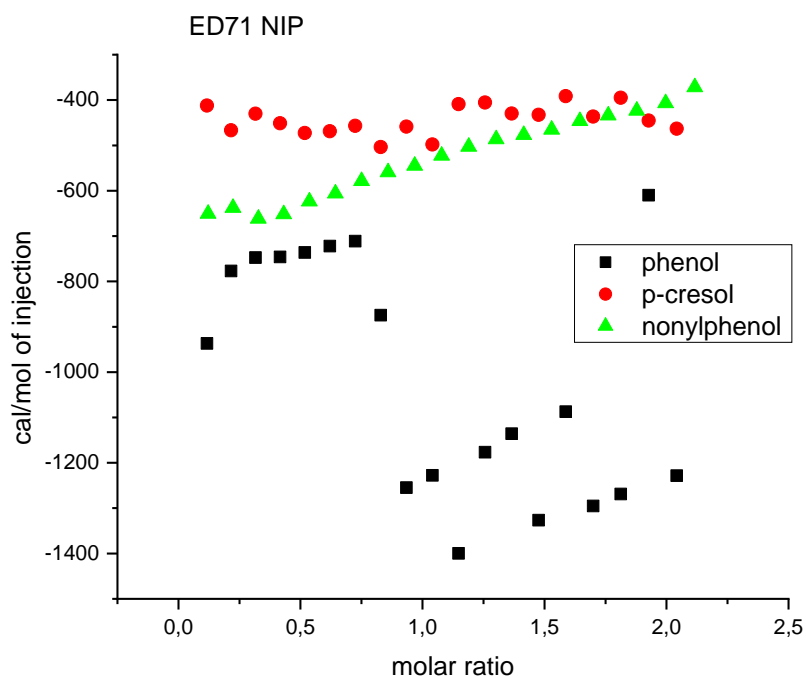
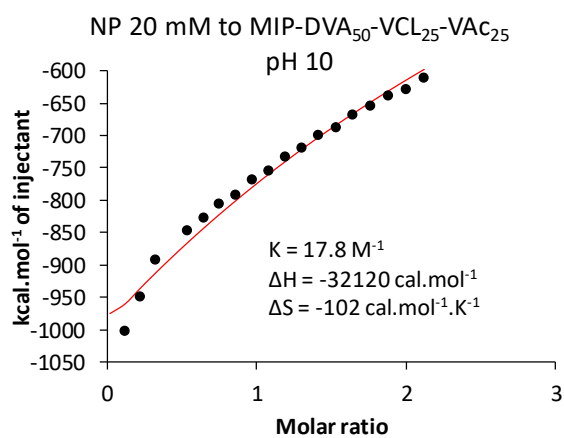
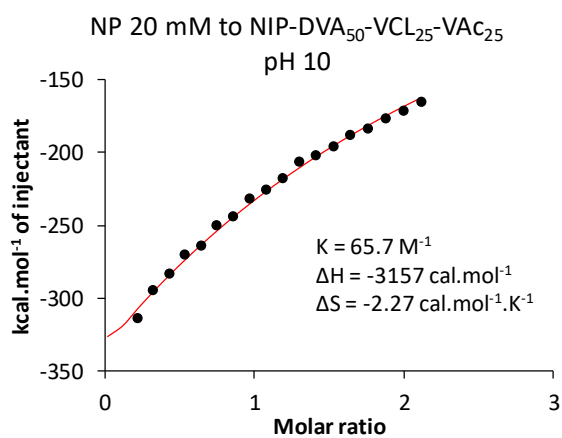


Figure S 22. Comparison of ITC traces for titration 20 mM of different injectants with NIP-DVA₅₀-VCL₂₅-VAC₂₅ at 5 g.L⁻¹ in ethanol/water 50/50 v:v at 25°C. Injectants are Nonylphenol, *p*-cresol and phenol.



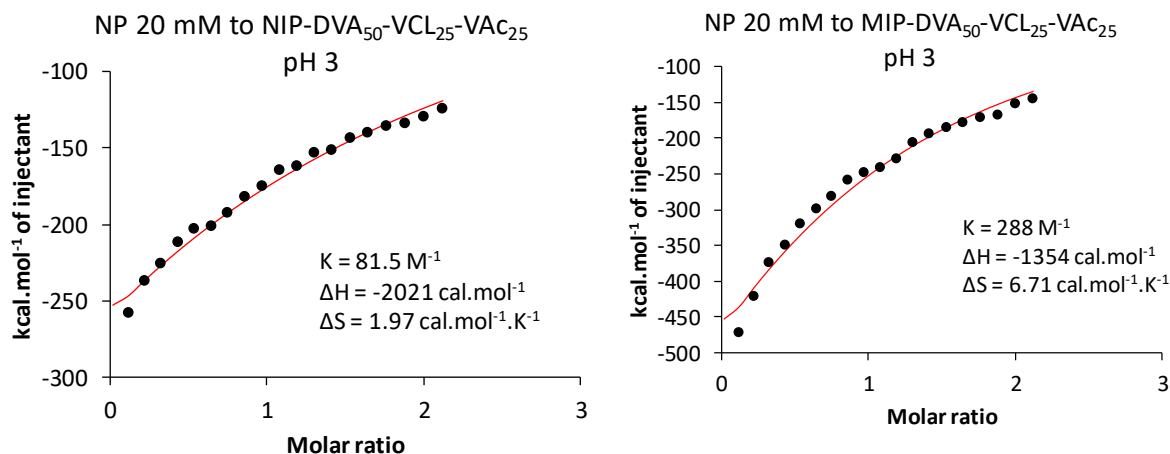


Figure S 23. Titration of 20 mM of nonylphenol with MIP-DVA₅₀-VCL₂₅-VAc₂₅ and NIP-DVA₅₀-VCL₂₅-VAc₂₅ at 5 g.L⁻¹ in ethanol/water 50/50 v:v at 25°C with water at pH10.7 (top) or pH 3 (bottom).

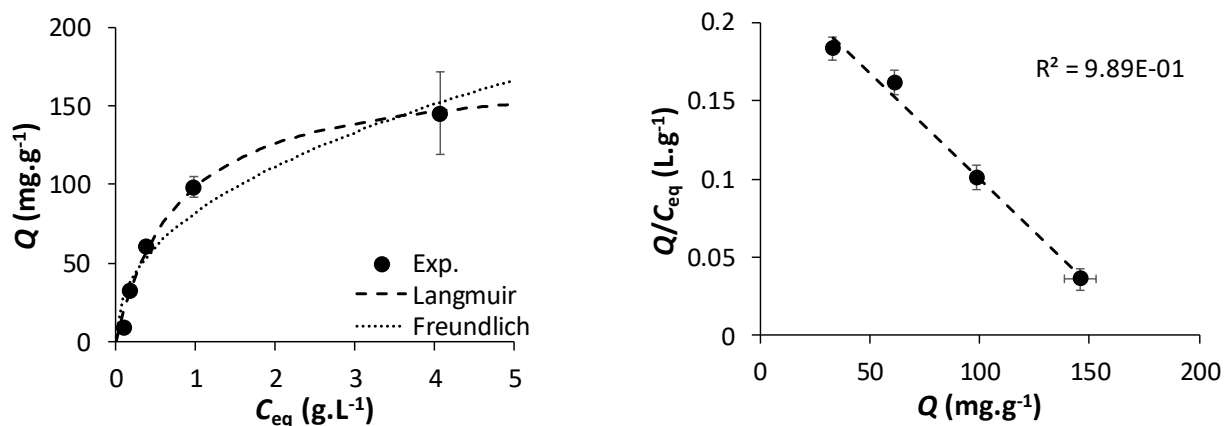


Figure S 24. Langmuir and Freundlich adsorption isotherm models (left) and corresponding Scatchard plots (right) for adsorption of NP onto MIP-DVA₆₆-VCL₁₇-VAc₁₇ carried out at room temperature in 50/50 (v/v) water/ethanol mixture. [MIP]₀ = 2.0 g.L⁻¹

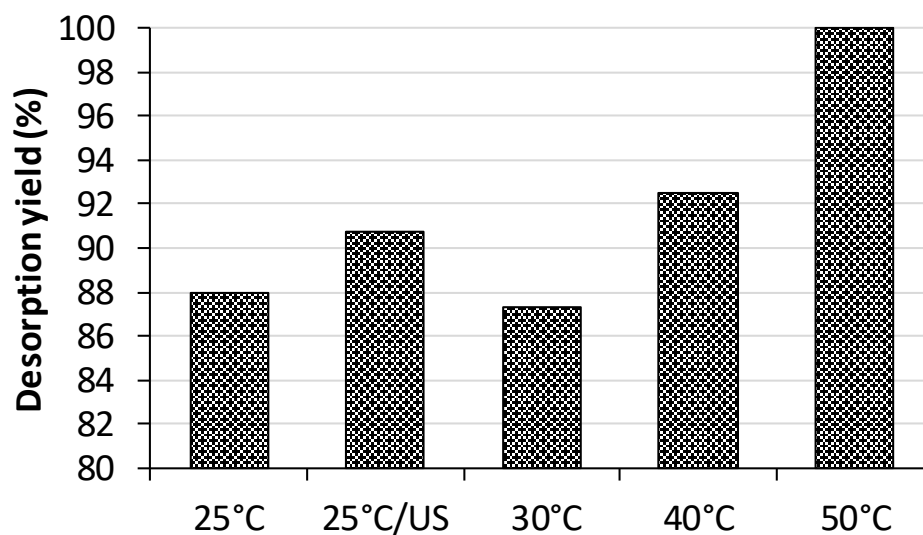


Figure S 25. Desorption yield of NP (calculated from Eq. S 7) for the MIP-DVA₆₆-VCL₁₇-VAc₁₇ in pure ethanol according to the temperature and the use of ultrasonication. US: ultrasonication.

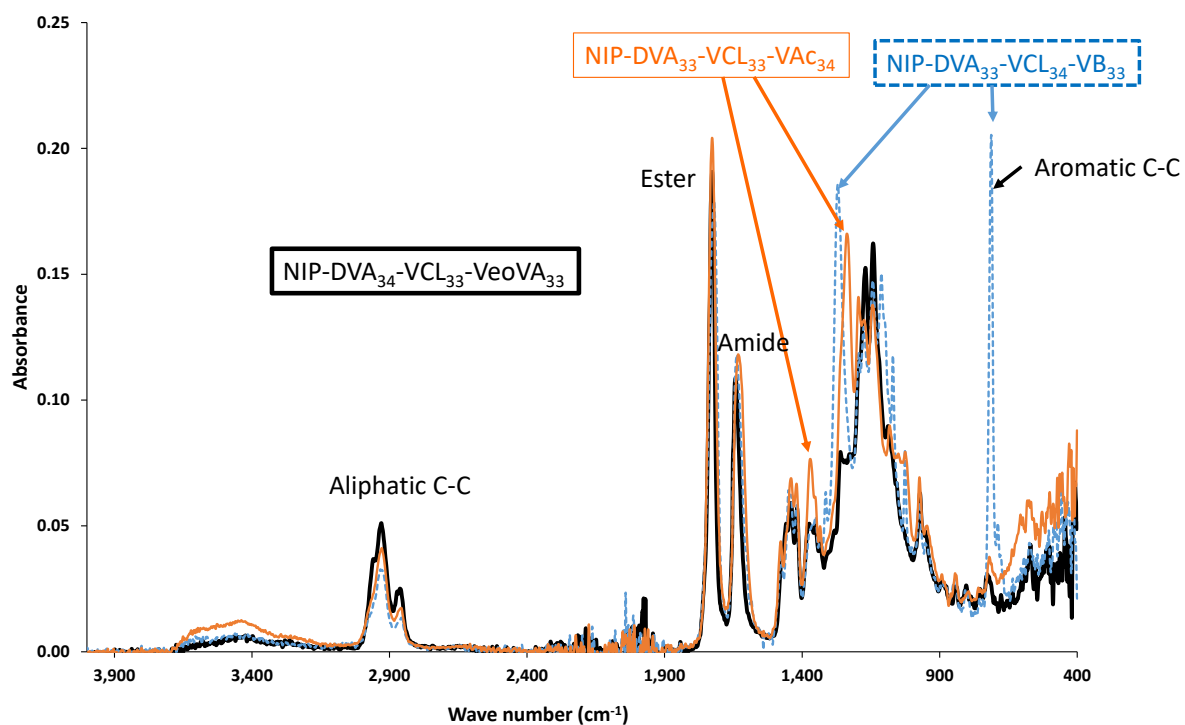


Figure S 26. FTIR spectra of NIP-DVA₃₃-VCL₃₃-VAc₃₄ (orange thin line), NIP-DVA₃₄-VCL₃₃-VeoVA₃₃ (Bold black line), NIP-DVA₃₃-VCL₃₄-VB₃₃ (Dotted blue line) in ATR mode.

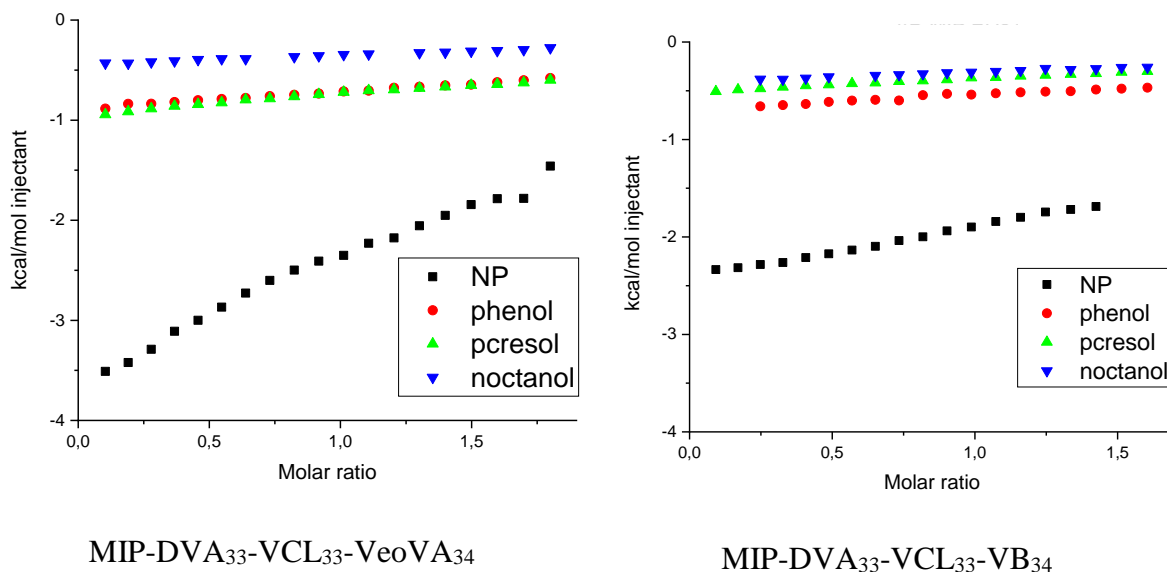


Figure S 27. Comparison of ITC traces for titration of NP (black squares), 1-octanol (inverse blue triangles), *p*-cresol (green triangle) and phenol (red dots) with MIP-DVA₃₄-VCL₃₃-VeoVA₃₃ (left) and MIP-DVA₃₄-VCL₃₃-VB₃₄ (right).

References

1. Gatidou, G.; Thomaidis, N. S.; Stasinakis, A. S.; Lekkas, T. D., Simultaneous determination of the endocrine disrupting compounds nonylphenol, nonylphenol ethoxylates, triclosan and bisphenol A in wastewater and sewage sludge by gas chromatography-mass spectrometry. *J Chromatogr A* **2007**, *1138* (1-2), 32-41.
2. Cavalheiro, J.; Monperrus, M.; Amouroux, D.; Preud'Homme, H.; Prieto, A.; Zuloaga, O., In-port derivatization coupled to different extraction techniques for the determination of alkylphenols in environmental water samples. *J Chromatogr A* **2014**, *1340*, 1-7.
3. Bizkarguenaga, E.; Iparragirre, A.; Navarro, P.; Olivares, M.; Prieto, A.; Vallejo, A.; Zuloaga, O., In-port derivatization after sorptive extractions. *J Chromatogr A* **2013**, *1296*, 36-46.
4. Imaz, A.; Miranda, J. I.; Ramos, J.; Forcada, J., Evidences of a hydrolysis process in the synthesis of N-vinylcaprolactam-based microgels. *European Polymer Journal* **2008**, *44* (12), 4002-4011.
5. Dossot, M.; Sylla, M.; Allonas, X.; Merlin, A.; Jacques, P.; Fouassier, J. P., Role of phenolic derivatives in photopolymerization of an acrylate coating. *Journal of Applied Polymer Science* **2000**, *78* (12), 2061-2074.